Synthesis and Photoisomerization of Divinyltetramethyldisiloxane and Divinyltetramethyldisilazane Complexes of (η^5-C_5R_5)Rh (R = H, Me). Crystal and Molecular Structure of (η^5-C_5Me_5)Rh[η^4-(CH_2=CH)$Me_2SiOSiMe_2$(CH=CH_2)]

Scott S. D. Brown,[1] Stephen N. Heaton,[2] Madeleine H. Moore,[2] Robin N. Perutz,*[,2] and Giles Wilson[2]

Research and Development, Dow Corning Ltd., Barry CF6 7YL, U.K., and Department of Chemistry, University of York, York YO1 5DD, U.K.

Received October 17, 1995[⊗]

The synthesis and photochemistry of a series of new rhodium complexes of 1,3-divinyl-1,1,3,3-tetramethyldisiloxane, (CH_2=$CHSiMe_2$)$_2$O, and its disilazane analogue (CH_2=$CHSiMe_2$)$_2$NH are reported. The divinyldisiloxane or divinyldisilazane ligands in (η^5-C_5R_5)Rh[η^4-(CH_2=$CHSiMe_2$)$_2$X] (R = H, Me; X = O, NH; type **1** complexes) are coordinated through the vinyl groups as for a diene. The structure of (η^5-C_5Me_5)Rh[η^4-(CH_2=$CHSiMe_2$)$_2$O] was established crystallographically. The two coordinated double bonds are arranged with their Si substitutents in a *cis* orientation with respect to the metal. The strain in the structure is suggested by the scissor geometry of the vinyl C=C bonds relative to the C_5 plane of the ring, combined with unequal Rh-C and C=C bond lengths. Photolysis of (η^5-C_5R_5)Rh(C_2H_4)$_2$ (R = H, Me) in the presence of (CH_2=$CHSiMe_2$)$_2$X (X = O, NH) results in the formation of the complexes of type **1**, together with an isomer in which the substituents on the coordinated C=C bonds are oriented *trans* at rhodium (**2**) and species containing two dangling divinyldisiloxane ligands, (η^5-C_5R_5)Rh[η^2-(CH_2=$CHSiMe_2$)$_2$X]$_2$, in both *cis* and *trans* configurations. Direct irradiation of species of type **1** converts them to the photoisomer **2**. The 16-electron intermediate with one η^2-divinyldisiloxane ligand may be trapped by addition of CH_2=$CHSiMe_3$ or excess (CH_2=$CHSiMe_2$)$_2$X (X = O, NH). The isomerization of type **2** species to type **1** species proceeds by first-order kinetics. For *trans*-(η^5-C_5H_5)Rh[η^4-(CH_2=$CHSiMe_2$)$_2$O] (**2a**) the values of $\Delta H^{\ddagger}$ and $\Delta S^{\ddagger}$ are 114 ± 1 kJ mol^{-1} and 41 ± 4 J mol^{-1} K^{-1}, consistent with rate-determining dissociation of one double bond. Replacement of C_5H_5 by C_5Me_5 increases $H^{\ddagger}$ by 9 ± 2 kJ mol^{-1}. The assignment of the photoisomers **2** as the *trans* species is supported by further observations that (i) a mixture of **1** and **2** can be synthesized by hydrolysis of chlorovinylsilane precursors (η^5-C_5H_5)Rh(η^2-CH_2=$CHSiMe_2Cl$)$_2$, a method which generates the Si−O−Si linkage in situ, (ii) the conformationally locked species with a cyclic trivinyltrimethyltrisiloxane ligand, (η^5-C_5H_5)Rh[η^4-(CH_2=$CHSi(Me)O$)$_3$], does not undergo photoisomerization, and (iii) the species with the Si−O−Si linkage replaced by a C−O−Si linkage (η^5-C_5H_5)Rh[η^4-(CH_2=CMe)CH_2OSiMe_2(CH=CH_2)] also fails to undergo photoisomerization. These complexes represent the first examples of adoption of a *trans* configuration at a metal by η^4-divinyldisiloxane ligands and the first examples of this type of isomerization.

Introduction

Transition-metal complexes with vinylsilane or vinylsiloxane ligands play an important role in the manufacture of silicones.[3,4] Karstedt's catalyst for hydrosilation contains the 1,3-divinyl-1,1,3,3-tetramethyldisiloxane ligand, (CH_2=$CHSiMe_2$)$_2$O, bound to platinum in a chelating and bridging fashion.[5] Following our studies of hydrosilation of ethene at rhodium(η^5-cyclopentadienyl),[6] we wished to investigate how the alkene moiety used in commercial systems would bind to this center. We chose as model ligands the divinyltetramethyldisiloxane and divinyltetramethyldisilazanes, (CH_2=$CHSiMe_2$)$_2$X (X = O, NH). Although many vinylsilane and vinylsiloxane complexes are now known,[7−17] few of these are half-sandwich complexes, e.g. (η^5-C_9H_7)Rh[η^4-(CH_2=CH)$_2$$SiMe_2$], CpCo[{1,2-$\eta^2$-

⊗ Abstract published in *Advance ACS Abstracts,* February 1, 1996.

(1) Dow Corning Ltd.

(2) University of York.

(3) Ookawa, S.; Yamada, S. Jpn. Patent JP 92-282533 920928. Waier, S. H.; Li, C-T.; Gyles-Mayon, D. U.S. Patent 93-133491 931007. Sato, R.; Yasuda, H. Jpn. Patent 92-242523 920820.

(4) Pan, J.; Lau, W. W. Y.; Lee, C. S. *J. Polym. Sci. A, Polym. Chem.* **1994,** *32,* 997.

(5) Hitchcock, P. B.; Lappert, M. F.; Warhurst, N. J. W. *Angew. Chem., Int. Ed. Engl.* **1991**, *30*, 438. Lappert, M. F.; Scott, F. P. A. *J. Organomet. Chem.* **1995**, *492*, C11.

(6) Duckett, S. B.; Perutz, R. N. *Organometallics* **1992**, *9*, 90.

(7) Christofides, A.; Ciriano, M.; Spencer, J. L.; Stone, F. G. A. *J. Organomet. Chem.* **1979**, *178*, 273.

(8) Isaeva, L. S.; Peganova, T. A.; Petrovski, P. V.; Kayumov, F. F.; Yusupova, F. G.; Yur'ev, V. P. *J. Organomet. Chem.* **1983**, *248*, 375.

(9) Lewis, L. N.; Colborn, R. E.; Grade, H.; Bryant, G. L.; Simpter, C. A.; Scott, R. A. *Organometallics* **1995**, *14*, 2202. Cloke, F. G. N.; Hitchcock, P. B.; Lappert, M. F.; MacBeath, C.; Mempsted, G. O. *J. Chem. Soc., Chem. Commun.* **1995**, 87.

0276-7333/96/2315-1392$12.00/0

Chart 1. Numbering of Complexes

(η^5-C_5R_5)Rh[η^4-(CH_2=$CHSiMe_2$)$_2$X] (**1** stable, **2** unstable)

(η^5-C_5R_5)Rh[η^2-(CH_2=$CHSiMe_2$)$_2$X]$_2$ (**3** t, **4** c)

(η^5-C_5R_5)Rh(η^2-CH_2=CH_2)[η^2-(CH_2=$CHSiMe_2$)$_2$X] (**5**)

(η^5-C_5R_5)Rh(η^2-CH_2=$CHSiMe_3$)[η^2-(CH_2=$CHSiMe_2$)$_2$X] (**6** t, **7** c)

(η^5-C_5R_5)Rh(PMe_3)[η^2-(CH_2=$CHSiMe_2$)$_2$X] (**8**)

Cp$Rh(\eta^2$-CH_2=$CHSiMe_2Cl)_2$ (**9** t, **10** c)

Cp$Rh(\eta^2$-CH_2=$CH_2)(\eta^2$-CH_2=$CHSiMe_2Cl)$ (**11**)

Cp$Rh[\eta^4$-(CH_2=$CHSiMe)_3(\mu$-$O)_3]$ (**12**)

Cp$Rh[\eta^4$-(CH_2=$CHSiMe_2$)(CH_2=$CMeCH_2$)O] (**13**)

a R = H, X = O **c** R = Me, X = O Cp = η^5-C_5H_5

b R = H, X = NH **d** R = Me, X = NH Cp* = η^5-C_5Me_5

t = *trans* c = *cis*

(cis-CH_3COCH=CH)}(η^2-CH_2=$CHSiMe_2$)],[18,19] and little photochemistry has been explored.

We report the synthesis and photochemistry of (η^5-C_5R_5)Rh[η^4-(CH_2=$CHSiMe_2$)$_2$X] complexes and show that they exist as two isomers which are interconverted photochemically. The structure of the more stable isomer of one species has been determined crystallographically. The unstable isomers have been characterized by multinuclear NMR spectroscopy and by several indirect methods: the generation of the same complexes by a hydrolytic route, comparisons to a complex with a cyclic trivinyltrisiloxane ligand, and comparison to an analogue with one silicon replaced by carbon. The kinetics of conversion of the unstable isomer to the stable one are shown to be consistent with initial dissociation of one arm of the chelate. We also report the formation of complexes containing two "dangling" divinyldisiloxane ligands, (η^5-C_5R_5)Rh[η^2-(CH_2=$CHSiMe_2$)$_2$X]$_2$, and several trapping products with one dangling ligand, (η^5-C_5R_5)Rh[η^2-(CH_2=$CHSiMe_2$)$_2$X]L (L = PMe_3, CH_2=$CHSiMe_3$, etc.). The compounds under study here are numbered in Chart 1.

Results

1. Synthesis of η^4-(CH_2=$CHSiMe_2$)$_2$X Complexes. Several new half-sandwich rhodium complexes of the form (η^5-C_5R_5)Rh[η^4-(CH_2=$CHSiMe_2$)$_2$X] (R = H, X = O (**1a**), NH (**1b**); R = Me, X = O (**1c**)) have been synthesized (Scheme 1). The procedure for **1a**,**b** was adapted from that for $CpRh(CH_2$=$CHSiMe_3)_2$.[20] At room temperature both complexes are air-stable orange oils, but **1a** crystallizes below 10 °C. Complex **1c** was prepared by a method similar to that used in the synthesis of $Cp^*Rh(C_2H_4)_2$.[21] Complex **1c** is an air, moisture, and light stable solid at room temperature. Crystals suitable for X-ray analysis were obtained.

Scheme 1. Synthesis of (a) 1a and 1b and (b) 1c

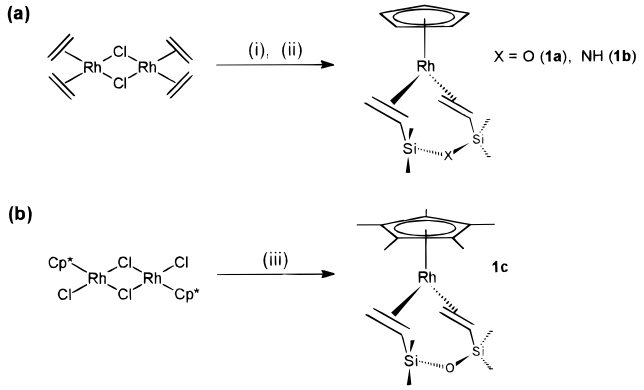

The complexes **1a**−**c** were characterized unambiguously by multinuclear NMR (Figure 1a, Table 1). The divinyl moiety of each is bound with a mirror plane containing the Rh−O vector, since the vinyls are magnetically equivalent, as are the $SiMe_2$ groups. Typically, a $^{29}Si\{^1H\}$ NMR spectrum contains just one $SiMe_2$ doublet which is shifted downfield from that of the free ligand by ca. 10 ppm, indicative of a vinylsilane bound to rhodium.[22] $^{13}C\{^1H\}$ NMR spectra contain two vinyl resonances ($J_{Rh-C} \approx 13-14$ Hz), which are assigned as either C^α (*C*H) or C^β (CH_2) on the basis of DEPT NMR experiments. Two signals due to $SiMe_2$ are detected; as the $SiMe_2$ groups show one ^{29}Si resonance, the methyls on each silicon must be inequivalent. Three vinyl resonances ($J_{Rh-H} \approx 1-3.5$ Hz) are observed in the ^1H NMR spectra, which are assigned as H^α (C*H*), H^β (CH_2-*trans*), or H^γ (CH_2-*cis*) from coupling constant data (see I for labeling).

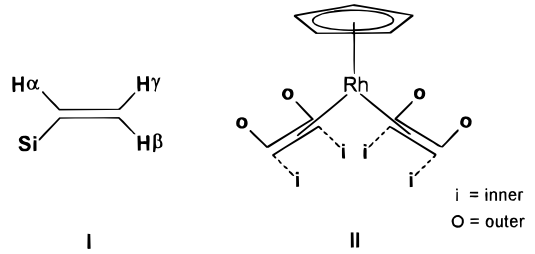

For **1a**,**b** the two CH_2 signals straddle that of the C*H* resonance. In accordance with Cramer's description of vinyl protons, the resonance at high field is assigned to the inner and those at low field to the outer protons (II).[23] Chelation forces H^α and H^γ to adopt outer

(10) Fitch, J. W.; Flores, D. P.; George, J. E. *J. Organomet. Chem.* **1971**, *29*, 263. Haschke, E. M.; Fitch, J. W. *J. Organomet. Chem.* **1973**, *57*, C93.
(11) Kelly, R. D.; Young, G. B. *J. Organomet. Chem.* **1989**, *361*, 123. Kelly, D. R.; Young, G. B. *Polyhedron* **1989**, *8*, 433.
(12) Haiduc, I.; Popa, V. *Adv. Organomet. Chem.* **1977**, *15*, 113.
(13) Schubert, U. *J. Organomet. Chem.* **1988**, *358*, 215. Schubert, U.; Grönen, J. *Organometallics* **1987**, *6*, 2458.
(14) Pearson, A. J.; Holder, M. S. *J. Organomet. Chem.* **1990**, *383*, 307. Paquette, L. A.; Daniels, R. G.; Gleiter, R. *Organometallics* **1984**, *3*, 560.
(15) Chow, T. J.; Cheng, C. C. *J. Organomet. Chem.* **1989**, *368*, 323.
(16) Fitch, J. W.; Ripplinger, E. B.; Shouldersand, B. A.; Sorey, S. D. *J. Organomet. Chem.* **1988**, *352*, C 25.
(17) Bandodokar, B. S.; Nagendrappa, G. *J. Organomet. Chem.* **1992,** *430***,** 373.
(18) Fitch, J. W.; Westmoreland, J. *J. Organomet. Chem.* **1984**, *268*, 269.
(19) Herberich, G. E.; Thönnessen, M. *J. Organomet. Chem.* **1979**, *177*, 357.
(20) Belt, S. T.; Duckett, S. B.; Haddleton, D. M.; Perutz, R. N. *Organometallics* **1989,** *8*, 748.
(21) Moseley, K.; Kang, J. W.; Maitlis, P. M. *J. Chem. Soc. A* **1970**, 2875.
(22) Bassindale, A. R.; Fitch, J. W.; Pannell, K. H. *J. Organomet. Chem.* **1981**, *209*, C65.
(23) Cramer, R. *J. Am. Chem. Soc.* **1964**, *86*, 217.

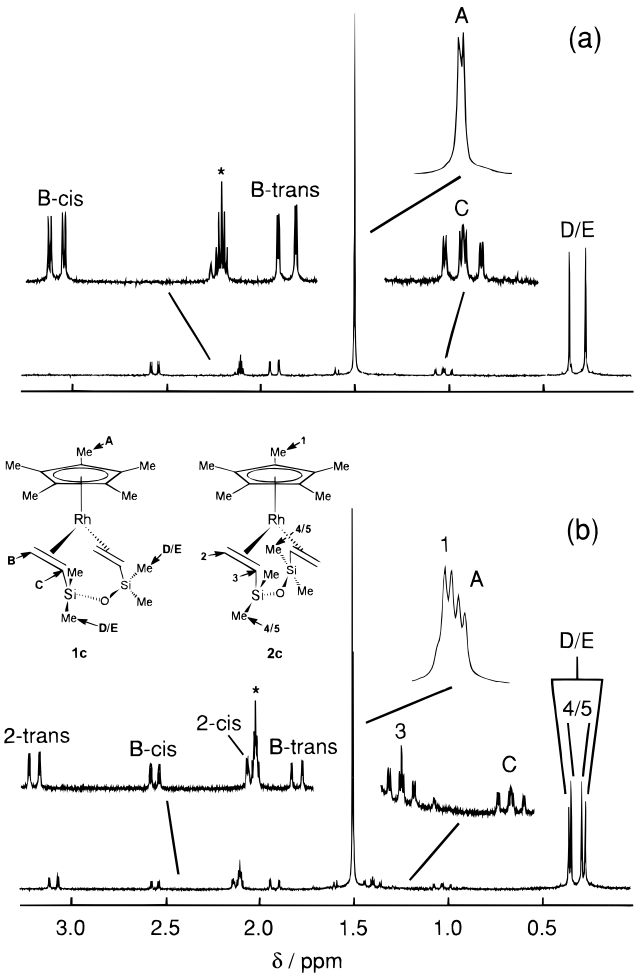

Figure 1. (a) ^{1}H NMR spectrum of **1c** in toluene-d_8 (* = solvent signal) at 293 K (protons labeled A−E). (b) Spectrum after irradiation showing formation of **2c** (protons labeled 1−5).

positions while, H^β lies at the inner position. For **1c** the vinyl resonance pattern is quite different. Proton H^α gives rise to the highest field signal of the three, while the resonance due to H^γ is at lowest field. An identical pattern is observed for the silazane analogue **1d**.

The fluxional behavior of (^{t}Bu$_3$P)Pt[η^4-(CH$_2$=CHSiMe$_2$)$_2$O] manifests itself in Si*Me*$_2$ signal broadening in the ^{1}H and ^{13}C{^{1}H} NMR spectra.[24] We acquired the ^{1}H NMR spectra of **1a** between 294 and 343 K, but no Si*Me*$_2$ signal broadening was observed. The rhodium−vinyl bond is sufficiently inert to prevent thermal vinyl dissociation. The inertness of **1a** was further confirmed by dissolving it in neat PMe$_3$. No reaction took place even after 15 h at room temperature.

2. Crystal Structure of 1c. The molecular structure of **1c** is shown in Figure 2a (Table 2). Notable features of the structure are as follows: (i) the Si substituents on the vinyl groups have a *cis* arrangement at the metal; (ii) a pseudo boat conformation is adopted by the divinyldisiloxane ligand as the vectors C(2)−Si(1), C(8)−Si(2), Si(1)−O, and Si(2)−O point away from the plane of the Cp* ring; (iii) the two methyl groups on each silicon atom are in pseudo axial and equatorial positions; (iv) the vinyl C=C bonds, C(1)−C(2) and C(7)−C(8), are tilted with respect to the C$_5$ plane of the Cp* ring in opposite directions by +6.2° and −8.9°, respectively; (v) the dihedral angle between planes containing rhodium, the centroid of the Cp* ring, and the center of each alkene C=C bond, α and β, is 5.5° (Figure 2b).

3. Photochemical Reaction of CpRh(C$_2$H$_4$)$_2$ with (CH$_2$=CHSiMe$_2$)$_2$X. We have shown previously that CpRh(C$_2$H$_4$)$_2$ is an excellent precursor for photoinduced substitution and oxidative addition reactions.[6,20] We therefore attempted to form **1a** and its analogues by photolysis of CpRh(C$_2$H$_4$)$_2$ in neat (CH$_2$=CHSiMe$_2$)$_2$X (X = O, NH). The four photoproducts formed from each precursor fall into two distinct categories: (i) those with one η^4-bound divinyl ligand, **1a**,**b** and **2a**,**b**, and (ii) those with two η^2-bound divinyl ligands, **3a**,**b** and **4a**,**b** (Chart 2). A typical product ratio was 3.7:3.8:1.5:1.0, respectively.

The assignment of η^2-vinyl coordination in **3** and **4** was made on the basis of NMR experiments (Table 3, Supporting Information). Both species contain two distinct types of vinyl groups. In the ^{1}H NMR spectrum one of these gives rise to a low-field ABC spin system and the other to a high-field AMX spin system. The AMX pattern results from a vinyl group bound to rhodium, while the ABC pattern is due to the uncoordinated vinyl group. Rotation about the Rh−vinyl bond can take place, resulting in broadening of NMR signals of **3** and **4** at 323 K. No chemical exchange occurs between the two at this temperature (^{1}H−^{1}H SECSY), indicating that they are noninterconverting isomers, both with two equivalent divinyl ligands. The major species, **3**, is assumed to have the silicon substituents arranged *trans* at the metal vinyl groups, while the minor isomer, **4**, has the *cis* structure (see below). The remaining two photoproducts have the divinyl ligand bound in a bidentate mode. The minor product of these is identified as a species of form **1**. We will show that the other, **2**, contains one chelating divinyl ligand which adopts a *trans* arrangement at the metal. When Cp*Rh(C$_2$H$_4$)$_2$ was irradiated in neat (CH$_2$=CHSiMe$_2$)$_2$X (X = O, NH), only two photoproducts were generated for each silicon precursor, both containing an η^4-divinyldisiloxane ligand. The minor product with X = O was identified as **1c**, and the other was a species of form **2c**. Similar complexes, **1d** and **2d**, were observed with X = NH.

Species **2a**−**d** are kinetic photoproducts which isomerize into **1a**−**d** over several days at room temperature. There are many differences between the NMR spectra of isomers of type **1** and those of type **2**, especially in signals due to the divinyldisiloxane ligand (Table 1). The ^{29}Si{^{1}H} NMR spectra of species of type **2** contain a doublet (typically, J_{Rh-Si} = 2 Hz) which is shifted downfield from that of **1** by ca. 3 ppm. A comparison of ^{13}C{^{1}H} NMR spectra shows that the chemical shift difference, δ, between the two vinyl carbons (C$^\beta$−C$^\alpha$) is much smaller in the case of **2** (Table 4). In the ^{1}H NMR spectrum of a species of type **2** the vinyl resonances are significantly shifted relative to those for **1** (Figure 3).

An intermediate photoproduct, CpRh(η^2-CH$_2$=CH$_2$)[η^2-(CH$_2$=CHSiMe$_2$)$_2$X] (X = O (**5a**), NH (**5b**)), is formed during the photochemical reaction between CpRh(C$_2$H$_4$)$_2$ and (CH$_2$=CHSiMe$_2$)$_2$X (Scheme 2, Table 3). Complex **5b** gives rise to two sets of vinyl resonances

(24) Bassindale, A. R.; Brown, S. S. D.; Lo, P. Y. *Organometallics* **1994**, *13*, 738.

Table 1. ^{1}H, ^{13}C{^{1}H}, and ^{29}Si{^{1}H} NMR Data for Species of Types 1 and 2 in Toluene-d_8 at 293 K

^{1}H NMR

species	C_5R_5 δ/ppm (J/Hz) R = H, Me	vinyl δ/ppm (J/Hz)[a] H$^\alpha$	H$^\beta$	H$^\gamma$	$SiMe_2$[b] δ/ppm
1a	d, 4.70 (J_{Rh-H} = 0.5, 5H)	ddd, 2.04 (J_{Rh-H} = 1.9, J_{trans} = 14.4, J_{cis} = 11.7, 2H)	dd, 1.66 (J_{Rh-H} = 1.2, J_{trans} = 14.4, 2H)	dd, 3.53 (J_{Rh-H} = 2.4, J_{cis} = 11.8, 2H)	s, 0.21 (6H); s, 0.38 (6H)
1b[c]	d, 4.75 (J_{Rh-H} = 0.7, 5H)	ddd, 1.99 (J_{Rh-H} = 1.7, J_{trans} = 14.7, J_{cis} = 11.5, 2H)	ddd, 1.66 (J_{Rh-H} = 1.4, J_{gem} = 0.6, J_{trans} = 14.3, 2H)	ddd, 3.56 (J_{Rh-H} = 2.5, J_{gem} = 0.6, J_{cis} = 11.5, 2H)	s, 0.13 (6H); s, 0.37 (6H)
1c	d, 1.50 (J_{Rh-H} = 0.5, 15H)	ddd, 1.03 (J_{Rh-H} = 1.7, J_{trans} = 14.3, J_{cis} = 11.5, 2H)	dd, 1.92 (J_{Rh-H} = 1.5, J_{trans} = 14.3, 2H)	dd, 2.54 (J_{Rh-H} = 2.3, J_{cis} = 11.7, 2H)	s, 0.27 (6H); s, 0.36 (6H)
1d[c]	d, 1.52 (J_{Rh-H} = 0.5, 15H)	ddd, 0.93 (J_{Rh-H} = 1.8, J_{trans} = 14.2, J_{cis} = 11.8, 2H)	dd, 1.94 (J_{Rh-H} = 1.4, J_{trans} = 14.2, 2H)	dd, 2.58 (J_{Rh-H} = 2.4, J_{cis} = 11.5, 2H)	s, 0.16 (6H); s, 0.37 (6H)
2a	d, 4.72 (J_{Rh-H} = 0.5, 5H)	ddd, 2.18 (J_{Rh-H} = 2.0, J_{trans} = 13.7, J_{cis} = 11.4, 2H)	dd, 2.78 (J_{Rh-H} = 1.8, J_{trans} = 13.9, 2H)	dd, 3.25 (J_{Rh-H} = 1.8, J_{cis} = 11.4, 2H)	s, 0.26 (6H); s, 0.37 (6H)
2b[c]	d, 4.78 (J_{Rh-H} = 0.7, 5H)	ddd, 2.17 (J_{Rh-H} = 1.9, J_{trans} = 14.0, J_{cis} = 11.2, 2H)	dd, 2.67 (J_{Rh-H} = 1.9, J_{trans} = 13.9, 2H)	dd, 3.25 (J_{Rh-H} = 1.9, J_{cis} = 11.2, 2H)	s, 0.11 (6H); s, 0.30 (6H)
2c	d, 1.50 (J_{Rh-H} = 0.5, 15H)	ddd, 1.40 (J_{Rh-H} = 2.2, J_{trans} = 13.5, J_{cis} = 11.2, 2H)	dd, 3.08 (J_{Rh-H} = 1.8, J_{trans} = 13.6, 2H)	dd, 2.12 (J_{Rh-H} = 1.8, J_{cis} = 11.2, 2H)	s, 0.29 (6H); s, 0.34 (6H)
2d[c]	d, 1.52 (J_{Rh-H} = 0.5, 15H)	ddd, 1.40 (J_{Rh-H} = 1.7, J_{trans} = 13.5, J_{cis} = 11.1, 2H)	dd, 3.05 (J_{Rh-H} = 1.7, J_{trans} = 13.4, 2H)	dd, 2.13 (J_{Rh-H} = 1.8, J_{cis} = 11.1, 2H)	s, 0.19 (6H); s, 0.31 (6H)

^{13}C{1H} and^{29}Si{^{1}H} NMR

species	^{13}C{^{1}H} NMR: $C^AC^B_5R_5$ (R = C^BH_3, H) δ/ppm (J/Hz) C^A	C^B	vinyl δ/ppm (J/Hz)[a,d] C^α	C^β	$SiMe_2$[b] δ/ppm	^{29}Si{^{1}H} NMR $SiMe_2$ δ/ppm (J/Hz)[f]
1a	d, 88.30 (J_{Rh-C} = 4.3)		d, 34.20 (J_{Rh-C} = 13.5)	d, 44.25 (J_{Rh-C} = 12.8)	s, 2.62; s, 3.91	d, 4.0 (J_{Rh-Si} = 2.1)
1b	d, 88.47 (J_{Rh-C} = 3.9)		d, 32.5 (J_{Rh-C} = 14.1)	d, 43.5 (J_{Rh-C} = 13.4)	s, 1.99; s, 3.45	d, 3.7 (J_{Rh-Si} = 2.0)
1c	d, 96.45 (J_{Rh-C} = 4.5)	s, 8.70	d, 41.90 (J_{Rh-C} = 14.2)	d, 51.6 (J_{Rh-C} = 14.2)	s, 2.20; s, 2.70	d, 3.2 (J_{Rh-Si} = 2.2)
1d	d, 95.81 (J_{Rh-C} = 4.2)	s, 8.18	d, 41.13 (J_{Rh-C} = 14.8)	d, 51.56 (J_{Rh-C} = 13.2)	s, 2.06; s, 3.68	d, 2.9 (J_{Rh-Si} = 2.0)
2a[e]	d, 88.75 (J_{Rh-C} = 4.1)		overlapping doublets, 34.91 (J_{Rh-C} = 13.3)		s, 2.92; s, 5.78	d, 6.3 (J_{Rh-Si} = 1.9)
2b[e]	d, 88.52 (J_{Rh-C} = 4.5)		overlapping doublets, 34.75 (J_{Rh-C} = 13.4)		s, 2.01; s, 4.44	d, 6.6 (J_{Rh-Si} = 1.6)
2c	d, 96.69 (J_{Rh-C} = 4.5)	s, 9.00	d, 42.30 (J_{Rh-C} = 15.3)	d, 44.1 (J_{Rh-C} = 13.2)	s, 2.40; s, 5.20	d, 5.9 (J_{Rh-Si} = 2.0)
2d	d, 96.06 (J_{Rh-C} = 4.3)	s, 8.43	d, 41.43 (J_{Rh-C} = 14.8)	d, 44.40 (J_{Rh-C} = 13.7)	s, 3.46; s, 5.52	d, 6.2 (J_{Rh-Si} = 1.7)

[a] Labeling: 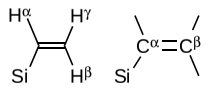 Assignments confirmed by 1H−1H COSY experiments in most cases. [b] Methyl groups in axial or equatorial positions could not be identified unambiguously.

[c] Signals due to N*H* could not be detected. [d] Spectral editing (DEPT) experiments were performed to confirm the vinyl carbon assignments. [e] The overlapping vinyl resonances gave rise to a broad doublet. Component signals could not be resolved by spectral editing. [f] A normal INEPT pulse sequence was employed.

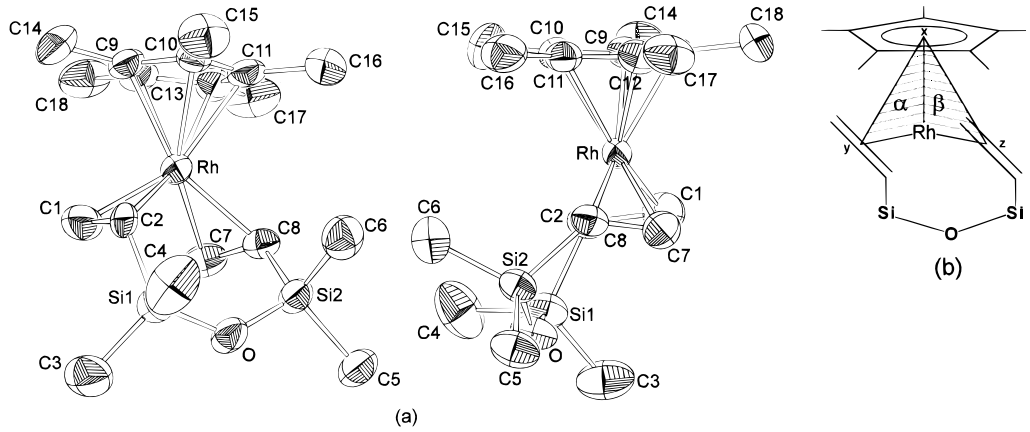

Figure 2. (a) Two ORTEP views of the crystal structure of **1c**. Anisotropic displacement ellipsoids are shown at the 50% probability level. (b) Representation of dihedral angle between planes α and β. Point x is the centroid of the Cp* ring. Points y and z are positioned at $^1/_2r$[(C(1)−C(2)] and $^1/_2r$[(C(7)−C(8)], respectively.

Table 2. Bond Lengths (Å) and Selected Bond Angles (deg) for 1c[a]

Rh−C(1)	2.115(5)	Si(1)−C(3)	1.867(7)
Rh−C(2)	2.180(5)	Si(1)−C(4)	1.866(7)
Rh−C(7)	2.133(5)	Si(2)−C(5)	1.869(5)
Rh−C(8)	2.154(5)	Si(2)−C(6)	1.852(6)
Rh−C(9)	2.208(4)	C(9)−C(10)	1.444(7)
Rh−C(10)	2.284(5)	C(9)−C(13)	1.430(7)
Rh−C(11)	2.269(5)	C(10)−C(11)	1.404(7)
Rh−C(12)	2.219(5)	C(11)−C(12)	1.430(7)
Rh−C(13)	2.242(5)	C(12)−C(13)	1.432(7)
C(1)−C(2)	1.436(7)	C(9)−C(14)	1.504(7)
C(7)−C(8)	1.400(7)	C(10)−C(15)	1.500(7)
Si(1)−C(2)	1.852(5)	C(11)−C(16)	1.512(7)
Si(2)−C(8)	1.850(5)	C(12)−C(17)	1.514(7)
O−Si(1)	1.641(4)	C(13)−C(18)	1.493(7)
O−Si(2)	1.637(4)		
Si(1)−O−Si(2)	132.0(2)	Rh−C(8)−Si(2)	117.9(2)
C(1)−Rh−C(2)	39.0(2)	O−Si(1)−C(2)	112.6(2)
C(7)−Rh−C(8)	38.1(2)	O−Si(2)−C(8)	109.7(2)
C(1)−Rh−C(7)	86.8(2)	C(10)−C(9)−C(13)	108.7(4)
C(2)−Rh−C(8)	100.2(2)	C(9)−C(10)−C(11)	107.4(4)
Si(1)−C(2)−C(1)	121.5(4)	C(10)−C(11)−C(12)	108.7(4)
Si(2)−C(8)−C(7)	126.1(2)	C(11)−C(12)−C(13)	108.6(4)
Rh−C(2)−Si(1)	125.0(2)	C(9)−C(13)−C(12)	106.5(4)

[a] Estimated standard deviations in the least significant figure are given in parentheses.

Chart 2. Structure of Species 1−4

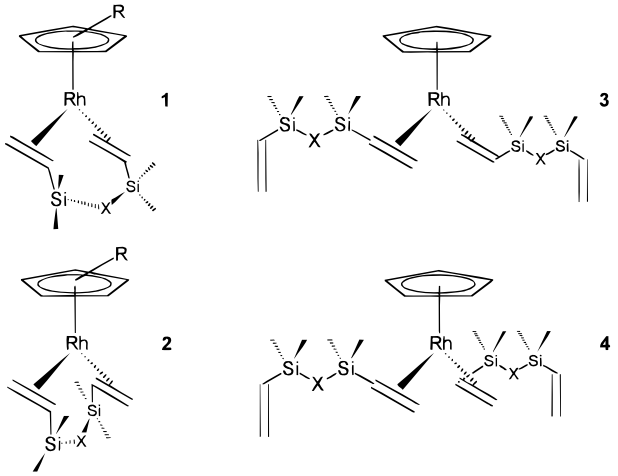

in the ^{1}H NMR spectrum which broaden on heating. The ^{13}C{^{1}H} NMR spectrum contains signals due to rhodium-bound ethene.

The photochemical reaction between CpRh(C_2H_4)$_2$ and (CH_2═$CHSiMe_2$)$_2$O in toluene-d_8 was monitored by ^{1}H NMR (Figure 4). At the photostationary state the product distribution (**1a**−**4a**) was the same as that observed in the reaction with neat siloxane. All photoproducts must themselves be photoactive. During irradiation a buildup and subsequent decay of **5a** takes place; the amount of free ethene in solution also increases.

Table 4. Difference between Vinyl Resonances in the ^{13}C{^{1}H} NMR Spectra of Species of Types 1 and 2[a]

species	$\Delta\delta(C^\beta - C^\alpha)$/ppm
1a	10.05
1b	11.00
1c	9.70
1d	10.43
2a	0
2b	0
2c	1.80
2d	2.97

[a] Conditions: 75.47 MHz; 298 K; toluene-d_8.

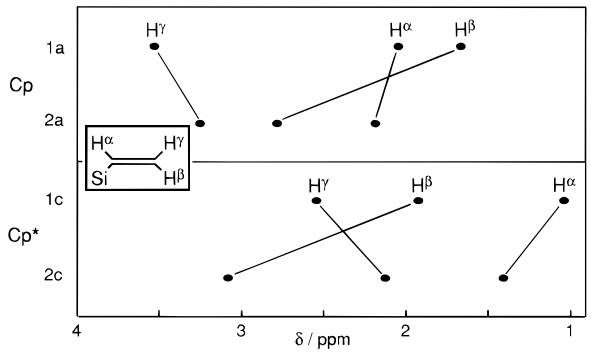

Figure 3. Relative chemical shifts of the vinyl protons in the ^{1}H NMR spectra of **1a, 2a, 1c, and 2c** (toluene-d_8, 293 K).

4. Direct Photolysis of 1a,c. The UV−visible spectra of **1a**,**c** contain maxima at the following values: λ_{max}/nm (ϵ/dm^3 mol^{-1} cm^{-1}) **1a**, 308 (4200), 414 (300); **1c**, 322 (6040), 421 (480). The lower energy bands extend well into the visible region. Irradiation (λ > 375 nm) of **1a** in neat (CH_2═$CHSiMe_2$)$_2$O generates a mixture of **1a**−**4a**, suggesting that photoinduced vinyl dissociation in **1a** results in a 16-electron species which is trapped by free vinylsiloxane. When the divinyldisiloxane is substituted by CH_2═$CHSiMe_3$, the major photoproducts are CpRh(η^2-CH_2═$CHSiMe_3$)[η^2-

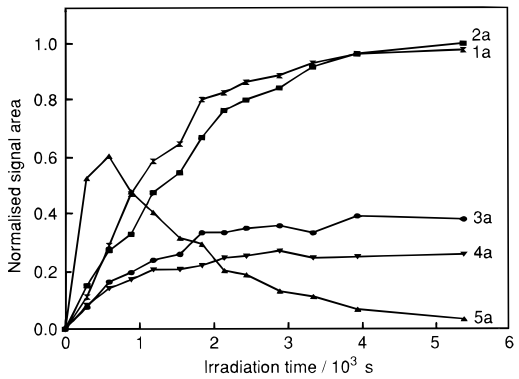

Figure 4. Variation of product distribution with irradiation time during photolysis of (η^5-C_5H_5)Rh(C_2H_4)$_2$ and (CH_2═$CHSiMe_2$)$_2$O in toluene-d_8 at 293 K. Relative concentrations are measured from the area of C_5H_5 resonances.

Scheme 2. Photochemical Reaction Mechanism Involved in the Formation of Species 1−4, the Photoisomerization of Species of Form 1, and the Trapping of the 16-Electron Intermediate

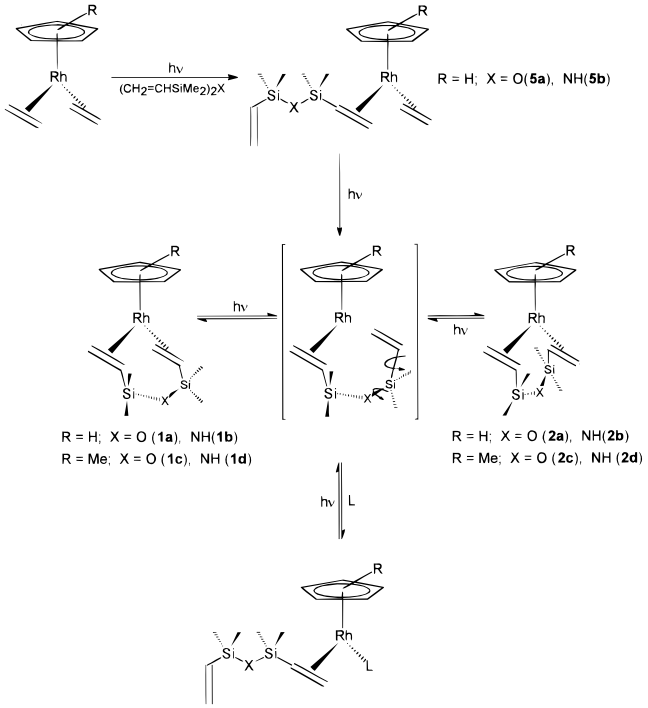

(CH_2═$CHSiMe_2$)$_2$O] (**6a**−**7a**, *cis* and *trans*, respectively) (Scheme 2, Table 5 (Supporting Information)). Trace amounts of **1a**,**2a** and CpRh(η^2-CH_2═$CHSiMe_3$)$_2$ (*cis* and *trans*) are also detected. Prolonged irradiation generates exclusively the latter.

Irradiation of **1a** in toluene-d_8 in the absence of free vinylsilane generates a mixture of **1a** and **2a** (**1a**:**2a** = 0.81:1 at the photostationary state) without any sign of decomposition. Irradiation of **1c** in toluene-d_8 generates a mixture of **1c** and **2c** in a ratio of 0.74:1 (Figures 1b and 5). When an equimolar mixture of **1a** (Cp) and **1c** (Cp*) was irradiated in toluene-d_8, only the photoisomerizations mentioned previously were observed, showing that species of type **2** are mononuclear. If dimer formation occurred on irradiation, a new Cp- and Cp*-containing product would be generated.

5. Kinetics of Isomerization of Complexes 2a−d to 1a−d. Species of type **2** isomerize thermally into **1**. The kinetics of this process were investigated for **2a**,**c**,**d**. Aliquots from stock toluene-d_8 solutions containing both **1** and **2** were monitored by ^{1}H NMR as they were maintained in the probe of the NMR spectrometer in the temperature range 305−340 K. All the species of type **2** were found to decay via a first-order process (Table 6, Figure 6). Values of $\Delta H^{\ddagger}$, $\Delta S^{\ddagger}$, and E_a were calculated from Eyring and Arrhenius plots. Substitution of NH for O in the divinyl backbone increases E_a insignificantly. Replacement of Cp by Cp* increases E_a and $\Delta H^{\ddagger}$ by 10 kJ mol^{-1}.

The thermal isomerization mechanism is thought to involve dissociation of a vinyl group from rhodium and its subsequent recoordination in a *cis* orientation relative to the other rhodium-bound vinyl group (Scheme 3). Trapping experiments were performed to confirm the initial cleavage of a rhodium−vinyl bond by allowing **2a** to react thermally in the presence of two-electron-donor ligands. ^{1}H NMR was used to monitor the thermal reaction between **1a**,**2a** and PMe_3 at 305 K. Species **2a** is slowly converted into the phosphine divinyldisiloxane complex CpRh(PMe_3)[η^2-(CH_2═$CHSiMe_2$)$_2$O] (**8a**) (Table 5), while the amount of

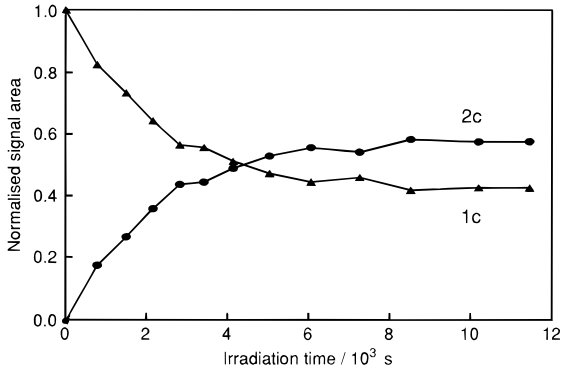

Figure 5. Variation of the concentrations of **1c** and **2c** during irradiation of **1c** in toluene-d_8 at 293 K. Concentrations are based on the area of the vinyl resonances.

Table 6. Rate Constants and Activation Parameters for the Thermal Isomerization of 2a,c,d in Toluene-d_8 at Various Temperatures[a,b]

system ([Rh]:[PMe_3])	temp/K	$k/10^{-5}$ s^{-1}
2a	305	3.0 ± 0.2
	313	8.2 ± 0.1
	320	27.0 ± 0.8
	328	70.0 ± 2.6
	336	198.0 ± 3.7
2c	310	6.9 ± 0.4
	315	16.0 ± 1.2
	320	30.0 ± 1.6
	325	68.0 ± 9.7
2d	313	3.6 ± 0.3
	320	9.3 ± 0.8
	330	39.0 ± 3.1
	340	172.0 ± 5.0
2a + PMe_3 (1:7)[c]	305	4.0 ± 0.2
2a + PMe_3 (1:12)[c]	305	4.1 ± 0.1

system	$\Delta H^{\ddagger}$/kJ mol^{-1}	$\Delta S^{\ddagger}$/J mol^{-1} K^{-1}	E_a/kJ mol^{-1}	log [A/s^{-1}]
2a	114 ± 1	41 ± 4	116 ± 1	15 ± 0.3
2c	123 ± 2	72 ± 8	126 ± 3	17 ± 0.3
2d	124 ± 2	66 ± 6	127 ± 2	17 ± 0.4

[a] An alcohol thermometer was used for temperature calibration. [b] 95% confidence limits. [c] In the presence of PMe_3, the product is **8a**, not **1a**.

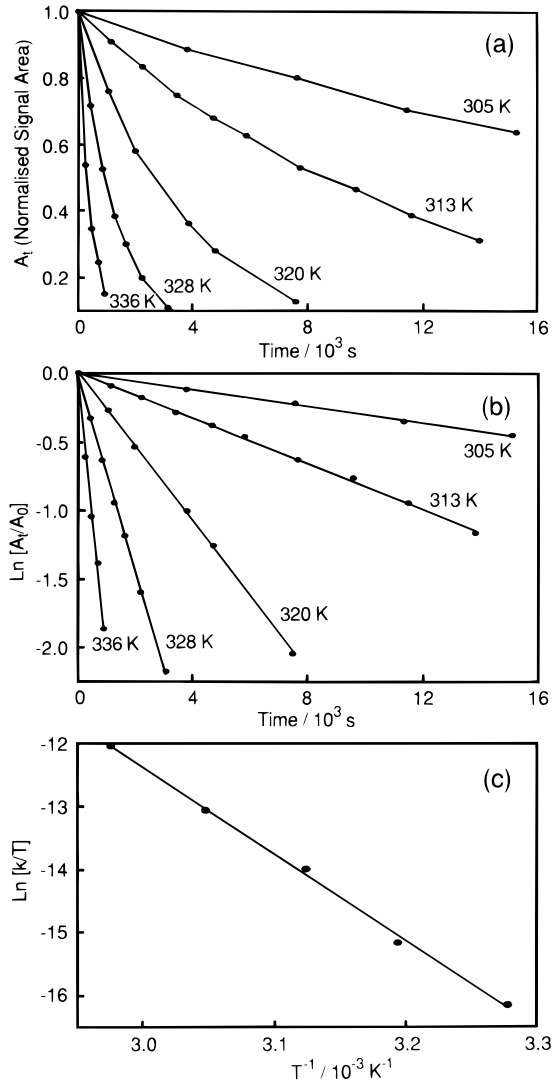

Figure 6. Thermal isomerization of **2a** into **1a** in toluene-d_8: (a) decay of a vinyl resonance of **2a** in the ^{1}H NMR spectrum with time, at various temperatures; (b) first-order plots for the decay of **2a**; (c) Eyring plot for the decay of **2a**.

1a in the system remains constant. The decay of **2a** is first order, with a rate independent of the [Rh]:[PMe_3] ratio. The rate constant was 4.0×10^{-5} s^{-1}, compared to 3.0×10^{-5} s^{-1} observed for the intramolecular thermal isomerization of **2a** to **1a** at this temperature. The identity of **8a** was confirmed by independent synthesis from CpRh(PMe_3)(C_2H_4). An analysis of the kinetics associated with the thermal isomerization mechanism (Scheme 3) yields the relationship for k_{obs} given by eq 1. With added PMe_3, the k_2 and k_{-1} steps become insignificant and $k_{obs} = k_1$.

$$k_{obs} = \frac{k_2 k_1}{(k_{-1} + k_2)} \qquad (1)$$

The rate constants measured at 305 K in toluene-d_8 yield the relationship $k_2 \approx 3k_{-1}$. This analysis shows that the rate of formation of **1a** from intermediate CpRh[η^2-(CH_2=$CHSiMe_2$)$_2$O] is 3 times greater than the rate of **2a** formation from this same precursor. Less effective trapping ligands were employed which did not prevent the isomerization of **2a** into **1a** completely. A mixture of **1a** and **2a** was dissolved in neat

Scheme 3. Mechanism of Thermal Isomerization of Species 2a−d into 1a−d and Trapping of the Coordinatively Unsaturated Intermediate

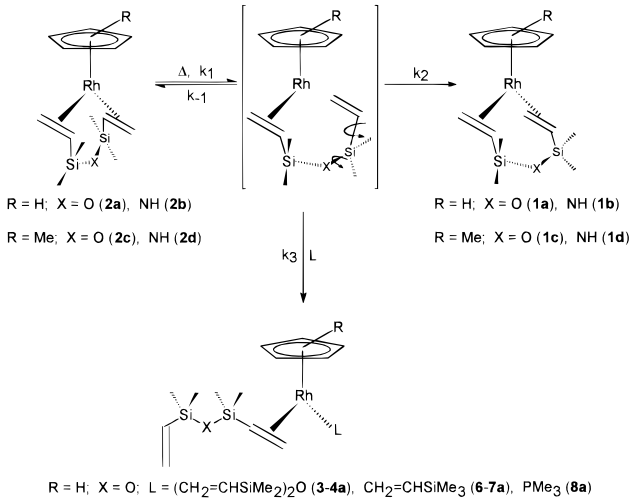

CH_2=$CHSiR'_2R$ (R′ = R = Me; R′ = Me, R = −$OSiMe_2$-CH=CH_2). Over several days at room temperature in the dark, **2a** was completely converted into **1a** and CpRh(η^2-CH_2=$CHSiR'_2R$)[η^2-(CH_2=$CHSiMe_2$)$_2$O] (*cis* and *trans*). Under the same conditions **1a** fails to react with CH_2=$CHSiR'_2R$.

6. Hydrolytic Synthesis of 1a and 2a. In order to test the hypothesis that the divinyl ligand in a species of type **2** has a *trans* vinyl configuration, **2a** and **1a** were synthesized from precursors which already contained vinyl ligands in *trans* and *cis* arrangements, respectively. By hydrolysis of CpRh(η^2-CH_2=$CHSiMe_2Cl$)$_2$ (**9** and **10**, *trans* and *cis*, respectively) a divinyldisiloxane ligand is formed within the coordination sphere of the metal. The vinyl groups remain bound to rhodium, while the two $SiMe_2Cl$ functionalities couple together.

The complex CpRh(η^2-CH_2=$CHSiMe_2Cl$)$_2$ was formed photochemically from the precursors CpRh(C_2H_4)$_2$ and CH_2=$CHSiMe_2Cl$. It was isolated as a moisture-sensitive yellow solid which contained the impurities CpRh(η^2-CH_2=CH_2)(η^2-CH_2=$CHSiMe_2Cl$) (**11**) and unreacted CpRh(C_2H_4)$_2$. Multinuclear NMR was used to identify **9**−**11** unambiguously (Table 5). The two methyls on each silicon are inequivalent, whereas the two vinyl groups are equivalent. Assignment of a *cis* (**10**) or *trans* (**9**) vinyl arrangement in the two bis(vinyl)-containing species was made on the basis of their relative proportions, as was the case for species of type **3** and **4**. The reaction of **9** and **10** with water in the presence of NEt_3 generated **2a** and **1a** respectively (Scheme 4). Only intramolecular ring closure is observed during hydrolysis. When the reaction was monitored by ^{1}H NMR in situ, we discovered that **9** has a half-life of ca. 20 min in the presence of water, while that of **10** is much longer, at several hours.

7. Synthesis of Analogues of 1 Which Cannot Undergo Photoisomerization. In a further test of the assignment of species of type **2** as a *trans* isomer of **1**, a complex with a rigid cage structure, **12**, was synthesized and tested for photoactivity (Table 5). This species contains a cyclic trivinyltrisiloxane ligand which is η^4-bound to rhodium. The Si^{α}−O−Si^{α} linkage between the chelating vinyl groups is held rigid by a second O−Si^{β}−O chain; thus, the formation of a *trans*

Scheme 4. Hydrolysis of Species 9 and 10

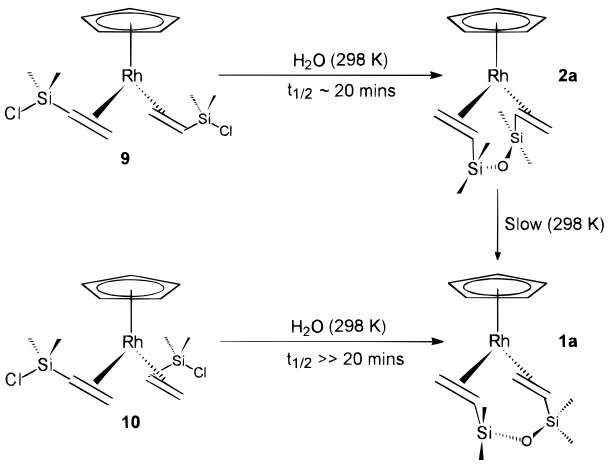

complex should be impossible. A toluene-d_8 solution of **12** was irradiated, but photoisomerization was not observed.

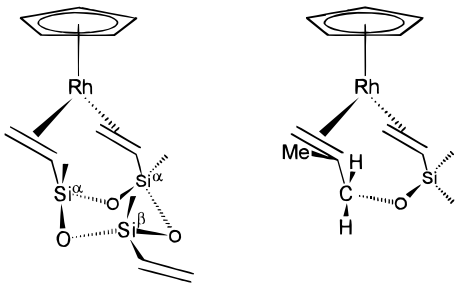

The *trans* bridge postulated for species of type **2** imposes considerable steric strain, as is shown by the conversion of **2a**−**d** into **1a**−**d**, respectively. An analogue of **2** with a shorter bridging group may well not be possible. With this reasoning in mind, a complex with a C−O−Si bridge, **13**, was synthesized (Table 5). In **13** the chelating bidentate ligand is an unsymmetrical allylvinylsiloxane. Irradiation of a toluene-d_8 solution of this species fails to produce a photoproduct. A control reaction was performed in which a toluene-d_8 solution containing an equimolar mixture of **13** and **1a** was irradiated. Only the photoisomerization of **1a** into **2a** was observed.

Trapping experiments were used to confirm that photoinduced rhodium-alkene bond cleavage does occur in **12** and **13**. Both species react photochemically with CH_2═$CHSiMe_3$ to give several products, none of which were characterized.

Discussion

1. Molecular Structure and NMR Spectra of Complexes of Type 1. Thermal and photochemical routes were used to synthesize species of type **1** from suitably active rhodium-containing precursors (Schemes 1 and 2). The crystal structure of **1c** (Figure 2a) shows that the divinyldisiloxane ligand adopts a conformation with vinyl groups linked *cis* at rhodium and both $SiMe_2$ groups in inner positions. An unexceptional Si−O−Si bond angle of 132.0(2)° results; cf. (^{t}Bu$_3$P)Pt[η^4-(CH_2═$CHSiMe_2$)$_2$O] (129.9(4)°) and [(Pt{η^4-(CH_2═$CHSiMe_2$)$_2$O}$)_2$(μ-(CH_2═$CHSiMe_2$)$_2$O)] (η, 136.0(1)°; μ, 134.7(8)°).[5,25] The mean rhodium−vinyl carbon bond length of 2.146 Å is in line with expectations; cf. CpRh(C_2H_4)$_2$ (2.109 Å) and (η^5-$C_9H_4Me_3$)Rh(C_2H_4)$_2$ (2.131 Å).[26,27] However, the difference in lengths of Rh−C(1) and Rh−C(2) (Δr(Rh−C) = 0.065(7) Å) combined with the difference in lengths of the C═C bonds (Δr(C−C) = 0.036(7) Å) and the scissoring of the C═C bonds by 15° is suggestive of strain imposed by the disiloxane bridge. For comparison, the differences in Rh−C and C═C bond lengths are much smaller in CpRh(η^4-COD) and Cp*Rh(η^2-CH_2═$CHCO_2Me$)$_2$ (maximum differences Δr(Rh−C) = 0.021 and 0.027 Å, Δr(C═C) 0.011(15) and 0.007(11), respectively). However, the scissoring in Cp*Rh(η^2-CH_2═$CHCO_2Me$)$_2$ is far larger.[28,29] In summary, strain in the structure of CpRh(η^4-COD) is much less severe than for **1c**. No corresponding structural perturbation is observed for (^{t}Bu$_3$P)Pt[η^4-(CH_2═$CHSiMe_2$)$_2$O].[25]

Only for **1c** can an unambiguous assignment of either a *cis* or *trans* vinyl arrangement at rhodium be made. Multinuclear NMR data for **1d** corresponds closely with that obtained for **1c**. Evidence to suggest that the divinyl moiety in **1a**,**b** has the same symmetry as that in **1c**, and not the alternative C_2 symmetry, comes from a study of photochemistry. Irradiation of **1a**−**d** generates the corresponding isomers **2a**−**d** (see below). For **1a** and **1c** the change in chemical shift for a particular vinylic proton is approximately the same on photoisomerization (Figure 3). We conclude that all species of type **1** have similar structures.

In the ^{13}C{^{1}H} NMR spectra of **1a**−**d** the vinylic carbon resonances are at much higher field than those of the free ligand. Similar upfield shifts have been reported in the spectra of Rh(I) complexes which contain either vinylsilane or allylvinylsilane ligands; this shift is more pronounced if the coordinated vinyl group is part of a chelating ligand.[30] For all species of type **1** the C$^\alpha$ resonance is at higher field than that of C$^\beta$. This is commonly observed for rhodium-bound chelating divinyl ligands, but for monodentate vinyl ligands the order is often reversed.

In the ^{1}H NMR spectra of **1a**−**d** unambiguous assignment of the vinylic proton H$^\alpha$ could be made, since this proton is coupled strongly to two others. The vinylic protons, H$^\beta$ and H$^\gamma$ were assigned on the basis of the standard assumption that $J_{trans} > J_{cis}$. In keeping with the structure proposed for these species, the resonances for **1a**,**b** due to H$^\beta$ are at higher field than those of H$^\alpha$ and H$^\gamma$, as described by Cramer.[23] This same resonance pattern has been reported for (acac)Rh[η^4-(CH_2═CH)$_2$-$SiMe_2$] and (η^5-C_9H_7)Rh[η^4-(CH_2═CH)$_2$$SiMe_2$] as well as for both alkene functions in the diallyl complex (acac)-Rh[η^4-(CH_2═$CHCH_2$)$_2$$SiMe_2$].[18,30]

The vinylic resonances in the ^{1}H NMR spectra of **1c**,**d** appear at positions contrary to those expected from the

(25) Chandra, G.; Hitchcock, P. B.; Lappert, M. F.; Lo, P. Y. *Organometallics* **1987**, *6*, 191.
(26) Blom, R.; Perutz, R. N.; Rankin, D. W. H.; Robertson, H. E. *J. Chem. Soc., Dalton Trans.* **1993**, 1983.
(27) Kakkar, A. K.; Taylor, N. J.; Calabrese, J. C.; Nugent, W. A.; Roe, D. C.; Connaway, E. A.; Marder, T. B. *J. Chem. Soc., Chem. Commun.* **1989**, 990.
(28) Adams, H.; Bailey, N. A.; Mann, B. E.; Taylor, B. F.; White, C.; Yavari, P. *J. Chem. Soc., Dalton Trans.* **1987**, 1947.
(29) Brookhart, M.; Calabrese, J. C.; Sabo-Etienne, S.; Fagan, P. J.; Garner, J. M.; Hauptman, E.; White, P. S. *J. Am. Chem. Soc.* **1994**, *116*, 8038.
(30) Fitch, J. W.; Osterloh, W. T. *J. Organomet. Chem.* **1981**, *213*, 493.

solid-state structure of **1c**. Although H^{α} and H^{γ} in both **1c** and **1d** occupy outer positions, they straddle the H^{β} resonance so that assignment of a vinylic proton as either inner or outer from chemical shift data is not possible. As shown below, the same is true for species of type **2**.

In contrast to related platinum complexes[5,24] the divinyldisiloxane ligand of **1a** is quite inert.

2. Photochemical Reactivity. In order to synthesize species of type **1** photochemically, bis(ethene) complexes (η^5-C_5R_5)Rh(C_2H_4)$_2$ (R = H, Me) were irradiated in (CH_2=$CHSiMe_2$)$_2$X (X = O, NH).[20,31,32] Four photoproducts (**1**−**4**) were formed from CpRh(C_2H_4)$_2$, and two (**1**, **2**) were formed from Cp*Rh(C_2H_4)$_2$, irrespective of the divinyl precursor used. In each case a photostationary state is reached with all products in photoequilibrium.

Species of type **2** are mononuclear and contain one chelating divinyl ligand (see below). The remaining photoproducts **3** and **4** are also mononuclear but contain two dangling η^2-bound divinyl ligands. The major isomer, **3**, has two ligands arranged *trans* at rhodium, while the minor isomer, **4**, has a *cis* structure. Brookhart *et al*. have reported that the thermal reaction between Cp*Rh(C_2H_4)$_2$ and CH_2=$CH(CO_2Me)$[29] yields two isomers of Cp*Rh(η^2-CH_2=$CH(CO_2Me)$)$_2$ in a ratio of 6:4. Brookhart *et al*. observe rotamers with inequivalent ligands, whereas **3** and **4** adopt rotameric conformations with ligands equivalent.[33] If one acrylate ligand in each of Brookhart's species were rotated about the metal−acrylate bond, *trans* and *cis* isomers would result with conformations equivalent to those we observe, with the *trans* isomer dominant. For all nonchelating bis(vinyl) complexes mentioned in this work, *cis* and *trans* isomers are assigned on the basis that the dominant isomer is always the *trans* species.

The photochemical reaction between CpRh(C_2H_4)$_2$ and (CH_2=$CHSiMe_2$)$_2$O yields a mono(ethene) complex, **5a**, prior to attainment of the photostationary state (Figure 4). The amount of **5a** peaks rapidly and then slowly falls to zero as irradiation progresses, suggesting that the eventual formation of **1a**−**4a** occurs via stepwise loss of ethene from the rhodium precursor. The mechanism of consumption of **5a** probably involves the photodissociation of ethene to give the 16-electron intermediate, CpRh[η^2-(CH_2=$CHSiMe_2$)$_2$O], with a dangling vinyl ligand which is then trapped by free divinyldisiloxane. Intermolecular vinyl coordination generates **3a** and **4a**, and intramolecular vinyl coordination forms **1a** and **2a**. The last two are the major species due to the chelate effect.

Irradiation of a toluene-d_8 solution of **1a** generates a mixture of **1a** and **2a**, with the latter being the major species at the photostationary state; an analogous result is obtained for **1c** (Figure 5, Scheme 1). The formation of a species of type **2** occurs via a photochemical intramolecular isomerization of **1**. For **1a** the photostationary state is reached after only 90 min of photolysis, whereas thermal equilibration at the same temperature takes days. Hence, the photoproducts are almost certainly photosensitive, themselves providing a pathway to regenerate **1a**. To confirm that we are examining an intramolecular process and not the formation of some dinuclear species, a toluene-d_8 solution containing equimolar quantities of **1a** and **1c** was irradiated. No new Cp- and Cp*-containing products were formed, implying that species of type **2** are mononuclear. The intermediate CpRh[η^2-(CH_2=$CHSiMe_2$)$_2$O] may be trapped by irradiation of **1a** in neat CH_2=$CHSiR'_2R$ (R′ = R = Me, R′ = Me, R = $OSiMe_2CH$=CH_2), yielding two isomeric forms of CpRh(η^2-CH_2=$CHSiR'_2R$)[η^2-(CH_2=$CHSiMe_2$)$_2$O] as well as **2a** (Table 5). This strongly suggests that the photoisomerization process is initiated by photoinduced rhodium−vinyl bond cleavage. In the absence of other two-electron-donor ligands the free vinyl group rebinds in one of two ways to give either a *cis* or *trans* vinyl arrangement at the metal.

Both **1a** and CpRh(C_2H_4)$_2$ react photochemically with (CH_2=$CHSiMe_2$)$_2$O to give **1a**−**4a**. The product distribution is the same at the photostationary state irrespective of the rhodium precursor used. As species of type **1** and **2** have been shown to be in photoequilibrium, this implies that species of type **3** and **4** must also be photoactive. In each of these systems the intermediate, CpRh[η^2-(CH_2=$CHSiMe_2$)$_2$O], is involved.

3. Structure of Complexes of Type 2 and Their Thermal Conversion to 1. Multinuclear NMR data are not sufficient to characterize species of type **2** unambiguously. However, they show that the divinyl ligand is chelating and is bound symmetrically to rhodium. As in complexes of type **1**, the two methyl groups on Si are inequivalent: $SiMe^aMe^b$. The difference in chemical shift between the vinylic ^{13}C resonances is substantially smaller than that observed for the corresponding species of type **1** (Table 4).

Assignment of the positions of vinylic protons as either inner or outer by considering only the relative chemical shifts of their signals can be misleading, as we have seen for species **1c**. We will adopt the simplest assumption, namely that each species of type **1** has the same structure and that the divinyl configuration in each species of type **2** is the same.

The kinetic investigation of the thermal isomerization of **2a** into **1a** gives insight into the source of strain that must exist in the divinyl ligand of **2** and, hence, into the structure of these species (Scheme 3). The rhodium−ethene bond strength in CpRh(C_2H_4)$_2$ is ca. 129 kJ mol^{-1};[34] the value of E_a for the isomerization of **2a** to **1a** is 116 ± 1 kJ mol^{-1}, consistent with the postulate that the rate-determining step of this decay is rhodium−vinyl bond cleavage. The value of E_a for the decay of **2c** is 10 kJ mol^{-1} greater than that measured for the decay of **2a**. Substitution of Cp for Cp* in **2c** increases the electron density at the metal center, resulting in a strengthening of the rhodium−vinyl bond. Activation parameters for the decay of **2c** and **2d** are effectively the same. The rate-determining step for the thermal isomerization is not influenced by the replacement of O by NH in the backbone.

When **2a** decays in the presence of a two-electron-donor ligand, L (L = PMe_3, CH_2=$CHSiR'_2R$ (R′ = R = Me; R′ = Me, R = -$OSiMe_2CH$=CH_2)) complexes of the

(31) Duckett, S. B.; Haddleton, D. M.; Jackson, S. A.; Perutz, R. N.; Poliakoff, M.; Upmacis, R. K. *Organometallics* **1988**, *7*, 1526.
(32) Bentz, P. O.; Ruiz, J.; Mann, B. E.; Spencer, C. M.; Maitlis, P. M. *J. Chem. Soc., Chem. Commun.* **1985**, 1374. Ruiz, J.; Mann, B. E.; Spencer, C. M.; Taylor, B. F.; Maitlis, P. M. *J. Chem. Soc., Dalton Trans.* **1987**, 1963.
(33) Cramer, R.; Reddy, G. S. *Inorg. Chem.* **1973**, *12*, 346.
(34) Cramer, R. *J. Am. Chem. Soc.* **1972**, *94*, 5681.

Chart 3. Configuration of 1 and Possible Configurations of 2

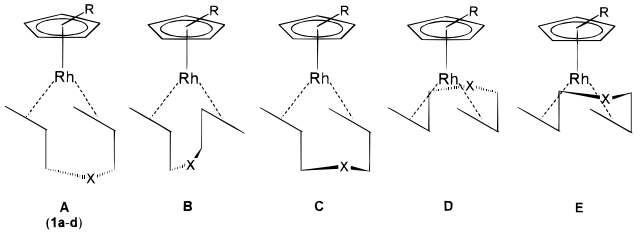

form CpRh[η^2-(CH_2=$CHSiMe_2$)$_2$O]L result. Trapping with PMe_3 completely prevents the isomerization of **2a** into **1a**; the thermally unstable complex is converted into CpRh(PMe_3)[η^2-(CH_2=$CHSiMe_2$)$_2$O] (**8a**) exclusively. The vinylsilane is a much less effective trapping agent; species **2a** decays in its presence to give **1a** together with traces of mixed vinyl complexes. These trapping experiments confirm not only that a rhodium−vinyl bond is cleaved during isomerization, yielding CpRh[η^2-(CH_2=$CHSiMe_2$)$_2$O], but also that the thermally stable isomer results from intramolecular ring closure within this 16-electron species.

In order to determine if thermal rhodium−vinyl bond cleavage in **2a** is reversible, ^{1}H NMR spectroscopy was used to monitor its decay in the presence of PMe_3 at 305 K. This allows the first-order rate constant, k_1, for the dissociation of a vinyl group from rhodium to be measured unambiguously. The rate of formation of **1a** from the intermediate is determined to be 3 times that for the formation of **2a** from the same intermediate; i.e., $k_2 \approx 3k_{-1}$.

There are four possible configurations in which the divinyldisiloxane ligand in **2a**−**d** could be symmetrically bound at rhodium (B−E; Chart 3). The structure of complexes of type **1** is shown as A.

The structures were modeled by taking the parameters of the crystal structure of **1c** and reconnecting bonds in the desired orientation followed by energy minimization. On the basis of the preceding thermal isomerization data, configuration C can be discounted, as thermal isomerization from a chair into a pseudo boat as in A would only involve the rotation of C−Si and Si−O bonds. Configurations D and E can also be ruled out. Molecular modeling shows that configurations D and E suffer several sources of steric strain: (i) in both there are methyl groups which approach close to the Cp ring; (ii) the tipping of the C−Si bonds in both D and E away from rhodium expands the Si···Si distance so as to strain the Si−O−Si bridge; (iii) the Si−O−Si bridge in D approaches close to rhodium and the Cp ring. This strain would probably result in enthalpies of activation for the thermal isomerization of **2a**−**d** lower than those actually observed. Molecular modeling of B shows that it has a slightly higher energy than that of A but demonstrates that the Si−O−Si linkage can bridge the *trans* positions and that the silicon-bound methyls lie outside the van der Waals radii of the Cp ring. This process gave a scale of steric strain in arbitrary units: A (0), B (6), C (79), D (119), E (122). Configuration B is the most likely to be adopted in species of type **2**.

In order to obtain conclusive evidence that the vinyl groups in **2a**−**d** adopt the *trans* geometry of type B, species **2a** and **1a** were generated from bis(vinyl)-

Chart 4. Views of Structures of Type 1 and 2 Adapted from Crystal Structure To Show Interconversion of Methyl Groups on Isomerization

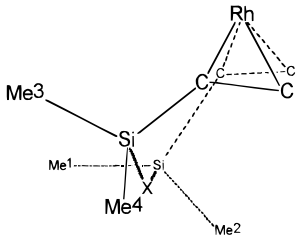

1

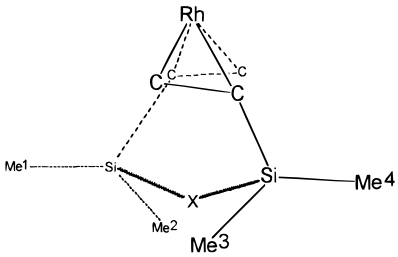

2

chlorosilane precursors with preassigned *trans* and *cis* vinyl arrangements, respectively. Two isomers of CpRh(η^2-CH_2=$CHSiMe_2Cl$)$_2$ (**9, 10**) result from the irradiation of CpRh(C_2H_4)$_2$ in CH_2=$CHSiMe_2Cl$. The vinyl arrangement in the major isomer (**9**) is assigned as *trans* and that in the minor isomer (**10**) as *cis* on the basis of ^{1}H NMR data (Table 5).

The reaction of Fe(CO)$_4$(η^2-CH_2=$CHSiMe_2Cl$) with water is known to generate a vinylsilanol complex and the dimeric species [(Fe(CO)$_4$)$_2$(μ-(CH=$CHSiMe_2$)$_2$O)] (see Note Added in Proof).[35] In contrast, hydrolysis of CpRh(η^2-CH_2=$CHSiMe_2Cl$)$_2$ causes only intramolecular ring closure. The reaction of **9** with water generates **2a** exclusively; hydrolysis of **10** gives only **1a**. The half-life for **9** was approximately 20 min, while that of **10** was several hours. We postulate a hydrolysis mechanism which involves rotation of vinyl groups about the rhodium−vinyl bond in **9** and **10** prior to ring closure. Different barriers to vinyl rotation would account for the differing rates of **1a** and **2a** formation.

One notable difference between the structure of a species of type **1** and that proposed for species of type **2** is that equivalent silicon-bound methyl groups in **1** become inequivalent in **2**, as shown in Chart 4. This follows because the isomerization of **1** into **2** involves Rh−vinyl bond cleavage followed by rotation of the free Si−vinyl carbon and Si−O bonds. The complex CpRh[η^4-(CH_2=$CHSiMe$)$_3$(μ-O)$_3$] (**12**) was synthesized, as it contains a chelating bidentate vinylsiloxane ligand, which can only adopt a *cis* arrangement at the metal. Equivalent positions at silicon are effectively locked together by a secondary siloxane linkage (Table 5).

The allylvinylsiloxane complex CpRh[η^4-(CH_2=$CHSiMe_2$)(CH_2=$CMeCH_2$)O] (**13**) was synthesized by the same procedure as that used to form **1a**,**b**. Species **13** is thermally stable and so is assumed to have a *cis* alkene arrangement at the metal. Substitution of CH_2

(35) Nurtdinova, G. V.; Pogrebnyak, A. A.; Rybin, L. V.; Rybinskaya, M. I.; Yur'ev, V. P. *J. Organomet. Chem.* **1981**, *217*, 373.

for $SiMe_2$ in the diene ligand backbone is estimated to reduce the length of the linkage between alkene groups by 0.8 Å compared to that in **1a**.[36] Molecular modeling suggests that the *trans* isomer of **13** would be considerably strained because of the short diene linkage.

The failure of both **12** and **13** to generate detectable photoisomerization products when irradiated provides further evidence that **2a**−**d** do indeed adopt a structure with two vinyl groups *trans* to one another.

In this discussion we made assumptions about the structures of the major and minor isomers of the nonchelating vinylsilane and vinylsiloxane complexes and that all species of type **1** are *cis* and those of type **2** are *trans*. Taken together, all evidence is consistent with these structural assignments.

Conclusions

Complexes of the type (η^5-C_5R_5)Rh[η^4-(CH_2=CH-$SiMe_2$)$_2$X] (R = H, Me; X = O, NH) exist in two isomeric forms which differ in their vinyl arrangements at the metal. The divinyldisiloxane ligand configuration in the less thermally stable of these, **2**, is unusual, as the vinyl groups are arranged with their substituents in *trans* positions with respect to the metal. The Si−X−Si bridge passes "across" the molecule with X in line with rhodium and the centroid of the C_5R_5 ring. To our knowledge this *trans* linkage between vinyl groups is the first of its kind. The thermally stable isomer **1** has a *cis* vinyl arrangement and a divinyl ligand configuration similar to that of the chelating vinylsiloxane ligand in (^{t}Bu_3P)-Pt[η^4-(CH_2=$CHSiMe_2$)$_2$O].[25] In the solid-state structure of **1c** there is some indication of strain in the divinyldisiloxane backbone.

Species of type **2** isomerize thermally into the corresponding species of type **1** via a mechanism which involves rhodium-vinyl bond cleavage as the rate-determining step. Irradiation of **1** regenerates **2**, again via a mechanism which is initiated by the dissociation of a vinyl group from the metal. The intermediate (η^5-C_5R_5)Rh[η^2-(CH_2=$CHSiMe_2$)$_2$X] is common to both these processes. The properties of disiloxane and disilazane analogues of species of type **1** are almost identical, as their vinyl group linkages are of similar length and flexibility. Complexes with chelating trivinyltrisiloxane or allylvinylsiloxane ligands fail to adopt *trans* ligand configurations when the linkage between the rhodium-coordinated alkenes is either much more rigid or much shorter.

Irradiation of **1a** or $CpRh(C_2H_4)_2$ in the presence of excess divinyldisiloxane ligand results in the formation of complexes with dangling divinyldisiloxane ligands in addition to formation of **2a**.

Experimental Section

General Considerations. All reactions were carried out under an inert atmosphere of argon with standard Schlenk techniques or a glovebox. Solvents were dried and distilled from sodium/benzophenone prior to use. Chromatography columns (10 cm length, 1.5 cm diameter) were packed with alumina (activated, neutral, 150 mesh). Unless otherwise stated, all reagents were purchased from Aldrich or Fluorochem Ltd. and used without further purification. [(C_2H_4)$_2$Rh(μ-Cl)]$_2$, [Cp*Rh(μ-Cl)Cl]$_2$, $CpRh(C_2H_4)_2$, Cp*Rh(C_2H_4)$_2$, and $CpRh(PMe_3)(C_2H_4)$ were prepared according to literature procedures.[20,21,37−39]

^{1}H (300 MHz), ^{13}C{^{1}H} (75 MHz), ^{29}Si{^{1}H} (59 MHz) (referenced to external TMS) and ^{31}P{^{1}H} (121 MHz) (referenced to external H_3PO_4) NMR spectra were recorded on a Bruker MSL 300 spectrometer in the solvent indicated. When integrations of Cp protons were required, delays of up to 150 s between pulses were employed for ^{1}H NMR spectra because of long T_1's. Similarly, delays of 60 s were used for ^{29}Si{^{1}H} NMR spectra, and around 700 scans were collected. The temperatures of NMR spectra were calibrated with an alcohol thermometer (<60 °C methanol, >60 °C glycol).[40] UV−visible spectra were recorded on a Perkin-Elmer Lambda 7 spectrophotometer. Mass spectra were recorded on a VG Autospec mass spectrometer. Desk Top Molecular Modeller was used in molecular modeling studies.[41] Elemental analysis was performed by Butterworths Laboratories.

The photolysis source was a Philips HPK 125 W medium-pressure mercury arc with a quartz focusing lens. Typically, a cutoff filter (λ > 375 nm or λ > 410 nm) was positioned in front of this lens. Photochemical reactions were carried out either in sealed 5 mm NMR tubes (Wilmad 507-PP) or in Pyrex ampules; both were fitted with a PTFE stopcock. Samples were suspended in a partially silvered Dewar containing distilled water (<10 °C) and irradiated through the walls of the Dewar.

Synthesis of CpRh[η^4-(CH_2=$CHSiMe_2$)$_2$X] (X = O (1a), NH (1b)). To a stirred solution of [(C_2H_4)$_2$Rh(μ-Cl)]$_2$ (1.3 mmol, 500 mg) in THF (20 mL) was added 2 equiv of (CH_2=$CHSiMe_2$)$_2$X over 10 min. After 20 min at ambient temperature, cyclopentadienylthallium (3.0 mmol, 0.81 g) was added and stirring continued for a further 3 h. The solvent was removed under vacuum to leave a dark brown solid residue, which was washed with hexane (2 × 20 mL). The resulting solution was eluted through an alumina column with a 50/50 (v:v) mixture of hexane and toluene. Solvent was evaporated in vacuo, and the resulting orange oil was sublimed at 30 °C, 4×10^{-3} mbar, onto a liquid-nitrogen-cooled finger. Both **1a** and **1b** were isolated as orange oils in 90% and 85% yield, respectively, based on rhodium. Neither these nor other oils were obtained in high enough purity to justify elemental analysis. Data for **1a** are as follows. Mass spec (EI) (*m*/*z* (%)): 354 (75), $[M]^+$; 339 (70), $[M - 15]^+$; 323 (30), $[M - 30]^+$; 168 (100), $[CpRh]^+$. Accurate mass (EI) (*m*/*z*): calcd for $C_{13}H_{23}$-$ORhSi_2$, 354.034 25; found, 354.034 30.

Synthesis of Cp*Rh[η^4-(CH_2=$CHSiMe_2$)$_2$O] (1c). To a suspension of [Cp*Rh(μ-Cl)Cl]$_2$ (0.49 mmol, 300 mg) and Na_2-CO_3 (2.1 mmol, 220 mg) in ethanol (40 mL) was added (CH_2=$CHSiMe_2$)$_2$O (1.0 mmol, 0.19 g). This mixture was stirred continuously for 3 h at 70 °C. The resulting pale yellow solution was cooled and filtered, and the solvent was removed under vacuum to leave a yellow oil. The oil was sublimed at 40 °C, 4×10^{-3} mbar, onto a liquid-nitrogen-cooled finger and recrystallized from a methanol and water mixture at −20 °C. Orange crystals of **1c** were isolated in 60% yield, based on rhodium. Anal. Calcd for $C_{18}H_{33}ORhSi_2$: C, 50.94; H, 7.78. Found: C, 50.68; H, 8.01. Mass spec (EI) (*m*/*z* (%)): 424 (25), $[M]^+$; 409 (7), $[M - 15]^+$; 394 (4), $[M - 30]^+$; 238 (100), $[Cp^*Rh]^+$. Accurate mass (EI) (*m*/*z*): calcd for $C_{18}H_{33}ORhSi_2$, 424.1125; found, 424.1120.

Synthesis of CpRh[η^4-(CH_2=$CHSiMe$)$_3$(μ-O)$_3$] (12). The method employed was identical with that used in the synthesis of **1a**. After sublimation the product was recrystallized from

(36) Atomic radii are taken from: Slater, J. C. *Quantum Theory of Molecules and Solids*; McGraw-Hill: New York, 1965; Vol. 2, Table 3−1.

(37) Cramer, R. *Inorg. Synth.* **1974**, *15*, 14.
(38) Moseley, K.; Kang, J. W.; Maitlis, P. M. *J. Am. Chem. Soc.* **1969**, *91*, 5970.
(39) Werner, H.; Feser, R. *J. Organomet. Chem.* **1982**, *252*, 351.
(40) Amman, C.; Meier, P.; Merbach, A. E. *J. Magn. Reson.* **1982**, *46*, 319.
(41) Appleyard, J.; Crabbe, C.; James, M. Desktop Molecular Modeller, Version 1.2; Oxford University Press: Oxford, U.K., 1989.

a methanol and water mixture at −20 °C. Yellow crystals of **12** were isolated in 70% yield based on rhodium. Mass spec (EI) (*m*/*z* (%)): 426 (100), $[M]^+$; 411 (7), $[M - 15]^+$; 396 (5), $[M - 30]^+$; 356 (45), $[M - 70]^+$; 168 (70), $[CpRh]^+$. Accurate mass (EI) (*m*/*z*): calcd for $C_{14}H_{23}O_3RhSi_3$, 426.0010; found, 426.0009.

Synthesis of (CH_2=$CHSiMe_2$)(CH_2=$CMeCH_2$)O. A two-neck, 1 L round-bottom flask was charged with CH_2=$CMeCH_2$-OH (64.0 mmol, 5.4 mL), NEt_3 (69.0 mmol, 9.6 mL), and Et_2O (100 mL) and cooled to 0 °C. The flask was then fitted with a 50 mL pressure-equalizing dropping funnel which contained CH_2=$CHSiMe_2Cl$ (66.4 mmol, 9.1 mL). Over 40 min the chlorosilane was added dropwise to the ether solution with continuous stirring. A white precipitate of (NEt_3H)Cl formed. The reaction vessel was warmed to room temperature and stirred for a further 15 h. The solution was filtered through Celite, and solvent was removed on a rotary evaporator. The product was distilled under reduced pressure into a liquid-nitrogen-cooled trap. A clear colorless liquid, free of impurities, was isolated in 100% yield, based on allyl alcohol. ^{1}H NMR spectrum (toluene-d_8, 293 K): 0.20 (s, 6H, SiMe_2), 1.70 (s, 3H, CH_2=C$Me$$CH_2$), 4.02 (s, 2H, CH_2=CMeCH_2), 4.82 (s, 1H, CH_2=CMeCH$_2$), 4.97 (s, 1H, CH_2=CMeCH$_2$), 5.79 (dd, 1H, J_{H-H} = 20.0, 5.7 Hz, SiCH=CH_2), 6.02 (s, 1H, J_{H-H} = 14.3, 5.7 Hz, SiCH=CH_2), 6.15 (dd, 1H, J_{H-H} = 20.0, 14.3 Hz, SiCH=CH_2).

Synthesis of CpRh[η^4-(CH_2=$CHSiMe_2$)(CH_2=$CMeCH_2$)O] (13). The method employed was identical with that used for **1a**. Species **13** was isolated as an orange oil in 82% yield, based on rhodium. Mass spec (EI) (*m*/*z* (%)): 324 (98), $[M]^+$; 309 (5), $[M - 15]^+$; 295 (8), $[M - 30]^+$; 283 (25), $[M - 41]^+$; 168 (100), $[CpRh]^+$.

Synthesis of CpRh(PMe_3)[η^2-(CH_2=$CHSiMe_2$)$_2$O] (8a). A Pyrex ampule was charged with CpRh(PMe_3)(C_2H_4) (0.18 mmol, 50 mg) and 10 equiv of (CH_2=$CHSiMe_2$)$_2$O (0.34 g); the volume of this mixture was made up to 3 mL by the addition of hexane. The resulting solution was thoroughly degassed and irradiated for 8 h with occasional agitation. Volatiles were removed in vacuo, and the resulting dark orange oil was redissolved in toluene. This solution was passed through an alumina column, eluting with toluene. The product was isolated as an orange oil in 86% yield, based on rhodium. Mass spec (EI) (*m*/*z* (%)): 430 (26), $[M]^+$; 354 (10), $[M - 76]^+$; 284 (9), $[M - 146]^+$; 244 (100), $[CpRh(PMe_3)]^+$; 168 (28), $[CpRh]^+$. Accurate mass (EI) (*m*/*z*): calcd for $C_{16}H_{32}OPRhSi_2$, 430.078 44; found 430.078 43.

Synthesis of CpRh(η^2-CH_2=$CHSiMe_2Cl$)$_2$ (9, 10). An ampule was charged with CpRh(C_2H_4)$_2$ (0.20 mmol, 45 mg) and hexane (1 mL) and CH_2=$CHSiMe_2Cl$ (3 mL). After degassing, the solution was irradiated for 7 h. All volatiles were evaporated in vacuo, giving a yellow solid which was purified by sublimation at 30 °C, 4×10^{-3} mbar, onto a liquid-nitrogen-cooled finger. A typical sample contained **9**, **10**, **13**, and CpRh(C_2H_4)$_2$ in a ratio of 1.0:0.81:0.23:0.08.

Photochemical Reaction of (η^5-C_5R_5)Rh(C_2H_4)$_2$ (R = Me, H) with (CH_2=$CHSiMe_2$)$_2$X (X = O, NH). Typically, an ampule was charged with 50 mg of (η^5-C_5R_5)Rh(C_2H_4)$_2$ and 3 mL of (CH_2=$CHSiMe_2$)$_2$X. The resulting solution was thoroughly degassed, cooled to <10 °C, and irradiated for no more than 6 h. Following the removal of volatiles under vacuum, the resulting orange oil was redissolved in hexane and the solution filtered through a pad of Celite. On evaporation of the solvent in vacuo an oil was isolated. Throughout the procedure the sample temperature was maintained at <10 °C.

Synthesis of Cp*Rh[η^4-(CH_2=$CHSiMe_2$)$_2$NH] (1d). The photochemical procedure above was used to generate a mixture of **1d** and **2d**. The resulting oil was heated in a water bath at 50 °C for 24 h, resulting in the complete conversion of **2d** into **1d**. Compound **1d** was isolated as an orange oil. Mass spec (EI) (*m*/*z* (%)): 423 (73), $[M]^+$; 408 (17), $[M - 15]^+$; 393 (5), $[M - 30]^+$; 238 (100), $[Cp*Rh]^+$. Accurate mass (EI) (*m*/*z*): calcd for $C_{18}H_{34}NRhSi_2$, 423.1284 85; found, 423.1283 62.

In Situ Monitoring of the Photochemical Reaction between CpRh(C_2H_4)$_2$ and (CH_2=$CHSiMe_2$)$_2$O. An NMR tube was charged with CpRh(C_2H_4)$_2$ (89.29 μmol, 20 mg) and toluene-d_8 (0.6 mL). To this solution was added 4 equiv of (CH_2=$CHSiMe_2$)$_2$O. After degassing, the mixture was irradiated and ^{1}H NMR spectra were acquired at regular intervals. A long delay between excitation pulses was employed, thus allowing reliable integration of the Cp resonances. During both irradiation and NMR acquisition the sample temperature was maintained at 16 °C.

Photoisomerization of 1a and 1c. An NMR tube was charged with approximately 50 μmol of either **1a** or **1c** and toluene-d_8 (0.6 mL). The tube was suspended in a partially silvered Dewar of distilled water, maintained at 16 °C. The mixture was irradiated, and ^{1}H NMR spectra were acquired at regular intervals.

Trapping of Intermediate in Photochemical Isomerization of 1a to 2a with CH_2=$CHSiR'_2R$ (R′ = R = Me; R′ = Me, R = −$OSiMe_2CH$=CH_2). Species **1a** (0.14 mmol, 50 mg) was placed in an ampule and dissolved in neat CH_2=$CHSiR'_2R$ (3 mL). This solution was degassed and irradiated for 3 h. The reaction mixture turned deep yellow but remained free of particulate material. All volatiles were removed under vacuum to give an orange oil.

Trapping of Intermediate in Thermal Isomerization of 2a to 1a with PMe_3 and CH_2=$CHSiR'_2R$ (R′ = R = Me; R′ = Me, R = −$OSiMe_2CH$=CH_2). A mixture of **1a** and **2a** was produced by irradiating **1a** (0.08 mmol, 30 mg) in hexane (3 mL) until a photostationary state was attained. Hexane was removed under vacuum, and the resulting orange oil was dissolved in either PMe_3 (3 mL) or CH_2=$CHSiR'_2R$ (3 mL). This solution was allowed to stand for 3 days in the dark, at ambient temperature. All volatiles were evaporated in vacuo to give an orange oil.

Hydrolysis of 9 and 10. An NMR tube was charged with toluene-d_8 (0.6 mL), NEt_3 (20 μL), and 20 mg of a typical mixture of **9**, **10**, **11**, and CpRh(C_2H_4)$_2$. After solution homogeneity was ensured, D_2O (40 μL) was added by syringe. The mixture was agitated to facilitate chlorosilane hydrolysis. ^{1}H NMR spectra were acquired at regular intervals after the addition of D_2O (298 K).

Thermal Isomerization Kinetics. (a) Sample Preparation. Species **1x** (**x** = **a**, **c**, **d**) (0.24 mmol) was placed in an ampule and dissolved in toluene-d_8 (3 mL). The solution was thoroughly degassed and irradiated for 6 h. Aliquots of 0.6 mL were taken from this stock solution and sealed in NMR tubes. These were stored at −78 °C prior to use.

(b) Monitoring of Isomerization. An NMR tube containing a mixture of **1x** and **2x** was placed in the preheated probe of an NMR spectrometer. The sample was allowed to equilibrate thermally for 5 min. ^{1}H NMR spectra were acquired at regular intervals until the conversion of **2x** into **1x** was complete.

Thermal Isomerization Kinetics in the Presence of PMe_3. (a) Sample Preparation. An ampule was charged with **1a** (0.11 mmol, 40 mg) and toluene-d_8 (1 mL), degassed, and irradiated for 6 h. The resulting mixture was split into two portions of equal volume (A and B). Two standard PMe_3 solutions were made up in toluene-d_8 (5 mL) (3.9 M and 6.8 M), and 0.1 mL of each was added to A and B respectively. These solutions were sealed in NMR tubes. The ratios of rhodium to phosphine in A and B were 1:7 and 1:12, respectively.

(b) Monitoring of Isomerization. An NMR tube containing a mixture of **1a**, **2a**, and phosphine was placed in the preheated probe of an NMR spectrometer (305 K). The sample was allowed to equilibrate thermally for 5 min. ^{1}H NMR spectra were acquired at regular intervals until the conversion of **2a** into **8a** was complete.

X-ray Crystal Structure of 1c. A yellow needle-shaped crystal was mounted on a glass fiber. Intensity data were collected on a Rigaku AFC6S four-circle diffractometer with

Table 7. Crystallographic Parameters for 1c

A. Crystal Data	
empirical formula	$C_{18}H_{33}ORhSi_2$
fw	424.53
habit, color, dimensions	yellow needle, $1.0 \times 0.30 \times 0.15$ mm^3
cryst syst	monoclinic
lattice type	P
no. of rflns used for unit cell determination (2θ range)	25 (22.0−25°)
ω scan peak width at half-height	0.25°
lattice params	$a = 15.177(6)$ Å $b = 7.681(6)$ Å $c = 18.376(7)$ Å $\beta = 93.76(4)°$ $V = 2138(2)$ Å^3
space group	$P2_1/c$ (No. 14)
Z	4
D_{calc}	1.319 g cm^{-3}
F_{000}	888.00
μ(Mo Kα)	9.11 cm^{-1}
B. Intensity Measurements	
diffractometer	Rigaku AFC6S
radiation	MoKα ($\lambda = 0.710\ 70$ Å), graphite monochromated
temp	293 K
cryst detector dist	40 cm
scan rate	2.0°/min (in ω) (2 rescans)
scan width	$(1.36 + 0.30 \tan\theta)°$
index ranges	$0 \le h \le 18$, $-5 \le k \le 9$, $-21 \le l \le 21$
θ range	2.52−25°
no. of rflns meas	total, 3959; unique, 3761 ($R_{int} = 0.0969$)
cor	Lorentz−polarization absorption (ψ scan) (transmissn factors 0.79−1.00) decay (−6.59% decline)
C. Structure Solution and Refinement	
structure soln	Patterson and Fourier expansion
refinement	full-matrix least squares on intensities, F^2
no. observns ($I > 3.00\sigma(I)$)	3705
no. of variables	199
rfln/param ratio	18.6
residuals	
R_F, wR_I ($I > 2\sigma(I)$)	0.0364, 0.1106
R_F, wR_I (all data)	0.0509, 0.3909
goodness of fit indicator on F^2	1.149
max peak in final diff map	0.939 e Å^{-3}
min peak in final diff map	−0/699 e Å^{-3}

graphite-monochromated Mo Kα X-radiation (Table 7). Accurate unit cell dimensions were obtained by a least-squares refinement of the values of 25 centered reflections in the range $22° < 2\theta < 25°$. Intensities of 3959 reflections were measured in the range $2.52° < \theta < 25.00°$ in a $\omega/2\theta$ scan mode. An empirical absorption correction based on azimuthal scans of four reflections was applied, resulting in transmission factors ranging from 0.79 to 1. Equivalent reflections were merged, and Lorentz and polarization corrections were applied. Atomic scattering factors were obtained from ref 42.

The structure was solved by Patterson and Fourier expansion techniques using DIRDIF92[43] and refined on intensities, F^2, using the refinement program SHELXL93.[44] All non-hydrogen atoms were refined anisotropically, and hydrogen atoms were refined using a rigid model (C_{sp^2}−H = 0.93 Å, C_{sp^3}−H = 0.96 Å) with $U_{iso}(H) = 1.2U_{eq}(C_{sp^2})$ and $U_{iso}(H) = 1.5U_{eq}(C_{sp^3})$. Atomic coordinates (Table 8, Supporting Information), and full-matrix least-squares refinement of 199 parameters for 3705 independent reflections ($I \ge \sigma(I)$) gave $R_F = 0.0509$ and w$R_I = 0.3909$ ($R_F = 0.0364$ and w$R_I = 0.1106$ on $I \ge 2\sigma(I)$ data). Full bond lengths and angles (Table 9), anisotropic displacement coordinates (Table 10), hydrogen coordinates and U_{eq} values (Table 11), and least-squares planes (Table 12) are given in the Supporting Information.

Note Added in Proof. In situ functionalization of a coordinated silyl group related to the conversion of **9** to **2a** has been described recently: Malisch, W.; Lankat, R.; Fey, O.; Reising, J.; Schmutzer, S. *J. Chem. Soc., Chem. Commun.* **1995**, 1917.

Acknowledgment. We acknowledge the support of the EPSRC, The European Commission, The Royal Society, and NATO. S.N.H. thanks Dow Corning Ltd. for their support. We appreciate valuable advice from Dr. S. B. Duckett.

Supporting Information Available: Tables of NMR data for complexes **3**−**13** and tables giving crystallographic data for **1c** (atomic coordinates, bond lengths and angles, anisotropic displacement parameters, hydrogen coordinates and U_{eq} values, least-squares planes) (13 pages). Ordering information is given on any current masthead page.

OM950826N

(42) Creagh, D. C.; McAuley, W. J. In *International Tables for Crystallography;* Wilson, A. J. C., Ed.; Kluwer Academic Publishers: Boston, MA, 1992; Vol C.

(43) Beurksens, P. T.; Admiraal, G.; Beurskens, G.; Bosman, W. P.; Garcia-Granda, S.; Gould, R. O.; Smits, J. M. M.; Smykalla, C. The DIRDIF Program System; Technical Report of the Crystallography Laboratory; University of Nijmegen: Nijmegen, The Netherlands, 1992.

(44) Sheldrick, G. M. SHELXL93, Program for the Refinement of Crystal Structures; University of Göttingen: Göttingen, Germany, 1995.